

*Supporting Information*

**Photobase-Catalyzed Thiol-ene Click Chemistry for Light-Based Additive Manufacturing**

Antonio Vazquez, Xabier Lopez de Pariza, Nathan Ballinger, Naroa Sadaba, Aileen Sun,  
Ayokunle Olanrewaju, Haritz Sardon and Alshakim Nelson\*

## Supplementary Information

### General Reagent Information

Aluminum oxide (activated, neutral, Brockmann I), 1-butyl-3-methylimidazole tetrafluoroborate ([BMIM] BF<sub>4</sub>, >98%), 1-vinylimidazole (>98.0%), 1-bromobutane (>99.0%), ethyl acetate (>99.7%), sodium tetrafluoroborate (98%), hexane (>99%), poly(ethylene glycol) diacrylate (PEGDA, M<sub>n</sub> = 575 g/mol) and trimethylolpropane tris(3-mercaptopropionate) (TMPTMP, 95.0%) were purchased from Sigma-Aldrich and used without further purification. Bromoethane (99.0%), 1-butylimidazole (98.0%), benzyltrimethylammonium hydroxide (Triton B, 40% in methanol), 1,8-diazabicyclo(5.4.0)undec-7-ene (DBU, 98.0%), lithium bis(trifluoromethanesulfonyl)imide (LiTFSI, 98.0%), paraformaldehyde (90.0%), sodium tetraphenylborate (98.0%), and 1,1,3,3-tetramethylguanidine (TMG, 99.0%) were purchased from Tokyo Chemical Industry and used without further purification. Dry tetrahydrofuran and dichloromethane were obtained from a Pure Process Technology purification system.

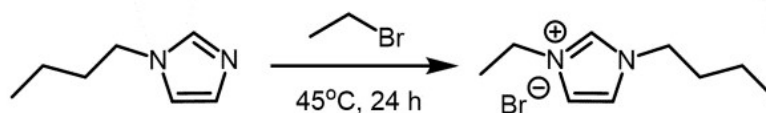
### General Analytical Information

<sup>1</sup>H NMR spectra were collected on a Bruker Avance 500 MHz spectrometer equipped with a Bruker triple resonance TXI probe and interfaced with a computer running Red Hat Enterprise Linux 6.3 and Topspin 2.1 software. <sup>13</sup>C NMR and <sup>19</sup>F NMR spectra were recorded on a Bruker Avance DRX499 spectrometer, equipped with a Bruker triple resonance BBO probe and interfaced with a computer running Red Hat Enterprise Linux 6.2 and Topspin 1.3 software. Rheology measurements were performed on a TA Discovery HR-2 Hybrid Rheometer. DSC measurements were performed on a TA Discovery DSC 2500 instrument. Electrical impedance spectroscopy (EIS) measurements were carried out on an Autolab 302N potentiostat galvanostat. Thermogravimetric analysis was conducted on a TA Q5000 thermogravimetric analyzer. 3D printed structures were printed using an Asiga Freeform Max UV-385 printer. Optical profilometry was collected using a Keyence VHX-970 digital microscope.

### Synthetic Procedure for Ionic Liquids

The general procedure for ionic liquid synthesis is based on previous work from our lab.<sup>1-3</sup>

*Synthesis of 1-butyl-3-ethyl imidazolium bromide* ([EBIM]Br):



**Scheme S1.** Synthetic route to 1-butyl-3-ethyl imidazolium bromide.

Under neat conditions, 1-butylimidazole (6.57 mL, 50 mmol) and bromoethane (4.48 mL, 60 mmol, 1.2 equiv.) were magnetically stirred at 45 °C for 24 h. After cooling, the viscous solution was washed with 50 mL ether five times and dried under vacuum to yield a clear viscous liquid ([EBIM]Br) in quantitative yield. <sup>1</sup>H NMR (500 MHz, DMSO-d<sub>6</sub>) δ 9.28 (s, 1H), 7.82 (dt, *J* = 9.0,

1.9 Hz, 2H), 4.24 – 4.14 (m, 5H), 1.78 (p,  $J = 7.3$  Hz, 2H), 1.42 (t,  $J = 7.3$  Hz, 3H), 1.26 (h,  $J = 7.4$  Hz, 2H), 0.90 (t,  $J = 7.4$  Hz, 3H).

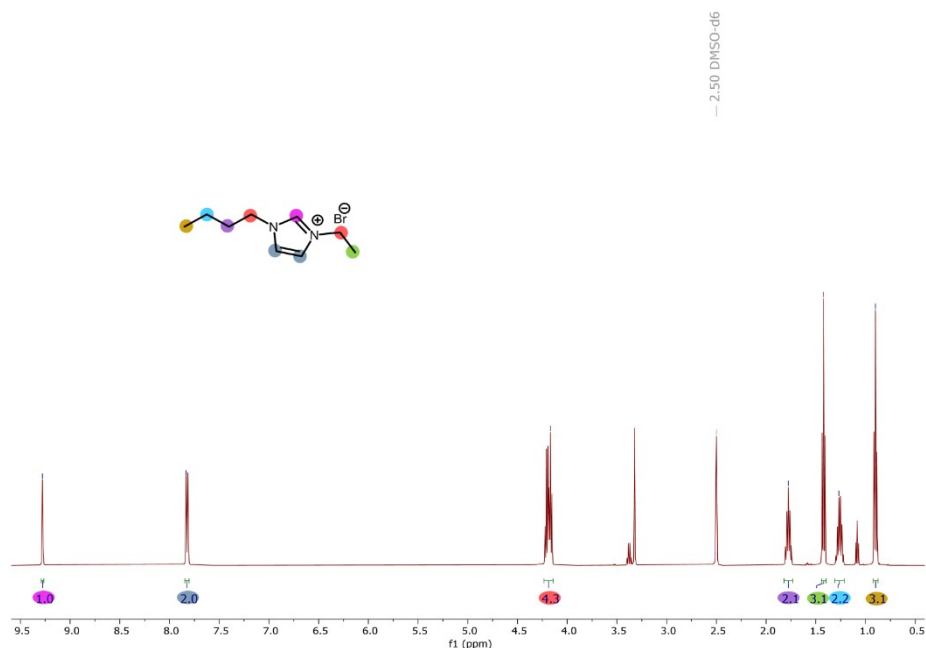
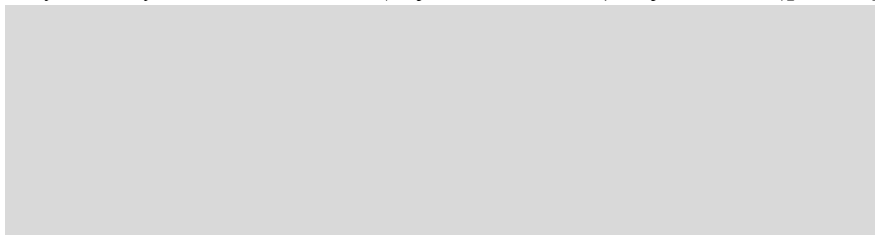


**Figure S1.**  $^1\text{H}$  NMR in DMSO- $d_6$  of [EBIM]Br.

*Synthesis of 1-butyl-3-ethyl imidazolium bis(trifluoromethane)sulfonimide ([EBIM]TFSI):*



**Scheme S2.** Synthetic route to 1-butyl-3-ethyl imidazolium bis(trifluoromethane)sulfonimide. Following this reaction, [EBIM]Br and lithium bis(trifluoromethane) sulfonimide (Li TFSI, 15.79 g, 55 mmol, 1.1 eq) salt were dissolved in 100 mL of DI water and stirred at room temperature for 48 hours. The biphasic mixture was separated with a separatory funnel and the ionic liquid layer was collected and passed through a plug of neutral alumina. The product was a clear liquid (Yield: 19.98 g, 92.2%).  $^1\text{H}$  NMR (500 MHz, DMSO- $d_6$ )  $\delta$  9.18 (s, 1H), 7.79 (dt,  $J = 8.9, 1.9$  Hz, 2H), 4.23 – 4.12 (m, 4H), 1.77 (p,  $J = 7.3$  Hz, 2H), 1.42 (t,  $J = 7.3$  Hz, 3H), 1.26 (h,  $J = 7.4$  Hz, 2H), 0.90 (t,  $J = 7.4$  Hz, 3H).  $^{19}\text{F}$  NMR (500 MHz, DMSO- $d_6$ ):  $\delta$  -78.7.  $^{13}\text{C}$  NMR (125 MHz, DMSO):  $\delta$  136.14, 122.89, 122.63, 121.25, 118.68, 49.05, 44.69, 31.77, 19.28, 15.45, 13.72

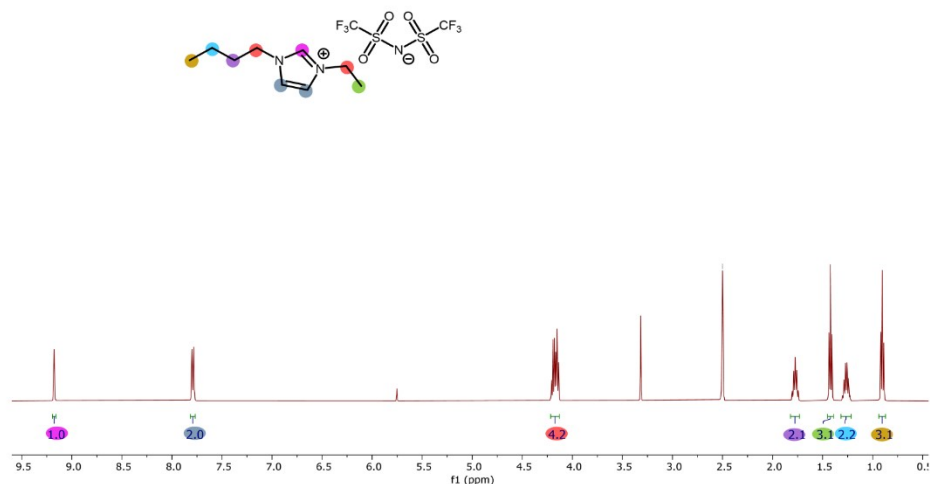


**Figure S2.** <sup>1</sup>H NMR in DMSO-d<sub>6</sub> of [EBIM]<sup>+</sup>TFSI<sup>-</sup>.

#### *Synthetic Procedure for Tetraphenylborate salts*

The tetraphenylborate salts were synthesized by adapting a previously published procedure.<sup>4</sup> The organic base, 1,8-diazabicyclo(5.4.0)undec-7-ene (10 mmol), was dissolved in 10 mL 10% HCl (aq) adjusting the pH to be greater than 3.0 to avoid decomposition of the NaBPh<sub>4</sub>. Next, a solution of NaBPh<sub>4</sub> (1.1 eq) in 10 mL of water was added to the base solution in water. The precipitate of the base salt was filtered, washed several times with water and then MeOH, and recrystallized from 4:1 mixture of MeOH:CHCl<sub>3</sub> and dried in vacuo.

<sup>1</sup>H NMR (500 MHz, DMSO) δ 7.18 (dddt, *J* = 6.6, 5.3, 2.7, 1.4 Hz, 8H), 6.93 (t, *J* = 7.4 Hz, 8H), 6.80 (t, *J* = 7.2 Hz, 4H), 3.55 – 3.49 (m, 2H), 3.44 (t, *J* = 5.9 Hz, 2H), 3.23 (dq, *J* = 6.1, 3.2 Hz, 2H), 2.65 – 2.59 (m, 2H), 1.89 (p, *J* = 5.8 Hz, 2H), 1.71 – 1.55 (m, 6H).

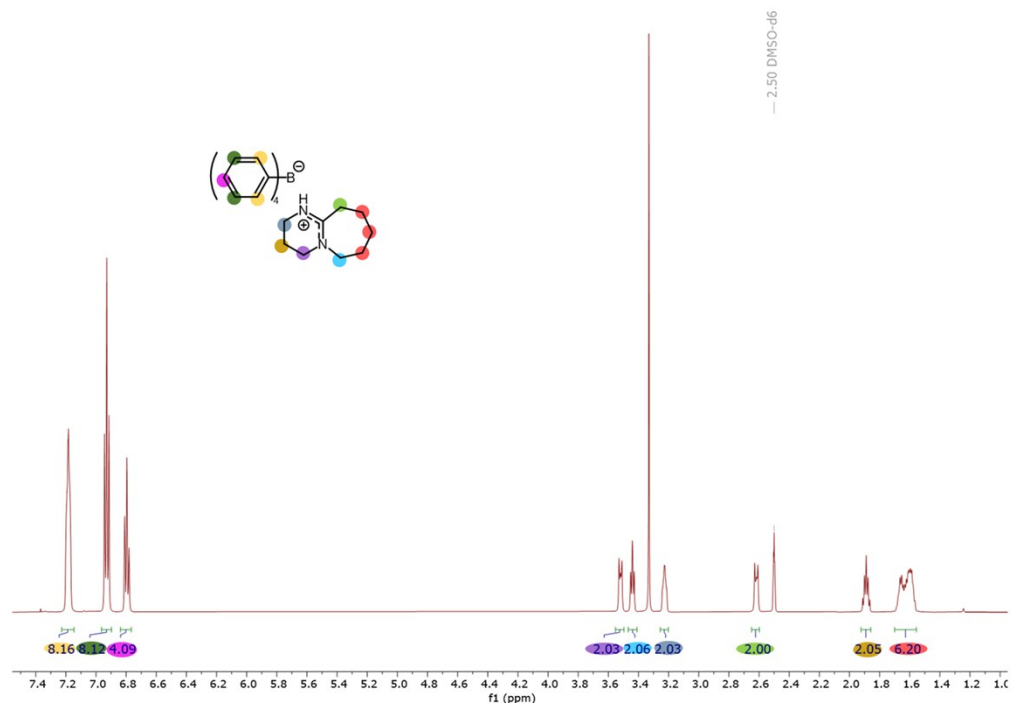
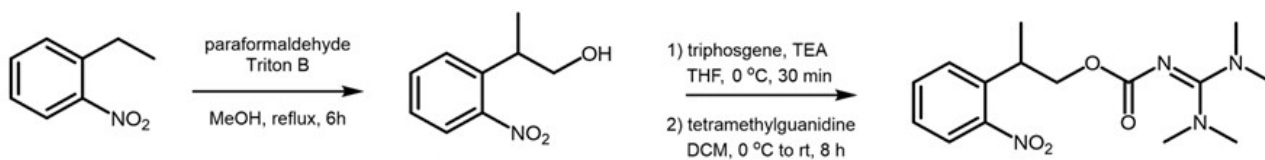


**Figure S3.**  $^1\text{H}$  NMR in  $\text{DMSO-d}_6$  of  $\text{DBU}\cdot\text{HBPh}_4$

*Synthetic Procedure for NPPOC-TMG*

The synthetic procedure was previously published.<sup>5,6</sup>



**Scheme S3.** Synthetic route for NPPOC-TMG.

Triton B (40% in MeOH, 3.0 mL, 6.6 mmol) was added to 2-ethylnitrobenzene (1.0 g, 6.6 mmol) and paraformaldehyde (0.20 g, 6.6 mmol), and the mixture was heated at reflux for 6 h. The reaction mixture was neutralized using 5% aqueous HCl. The mixture was extracted with ethyl acetate ( $3\times 10$  mL), dried over  $\text{MgSO}_4$ , and concentrated at reduced pressure. The residue was purified by flash chromatography using hexane–ethyl acetate (4:1) to give 2-(2-nitrophenyl)propanol (53%, red oil).  $^1\text{H}$  NMR (500 MHz,  $\text{CDCl}_3$ )  $\delta$  7.75 (dd,  $J = 8.2, 1.4$  Hz, 1H), 7.57 (td,  $J = 7.6, 1.3$  Hz, 1H), 7.49 (dd,  $J = 8.0, 1.5$  Hz, 1H), 7.36 (ddd,  $J = 8.5, 7.4, 1.4$  Hz, 1H), 3.79 (t,  $J = 7.1$  Hz, 2H), 3.52 (h,  $J = 6.8$  Hz, 1H), 1.64 (s, 1H), 1.33 (d,  $J = 6.9$  Hz, 3H).  $^{13}\text{C}$  NMR (125 MHz,  $\text{CDCl}_3$ )  $\delta$  150.75, 138.12, 132.65, 128.22, 127.20, 124.10, 67.85, 36.39, 17.55.

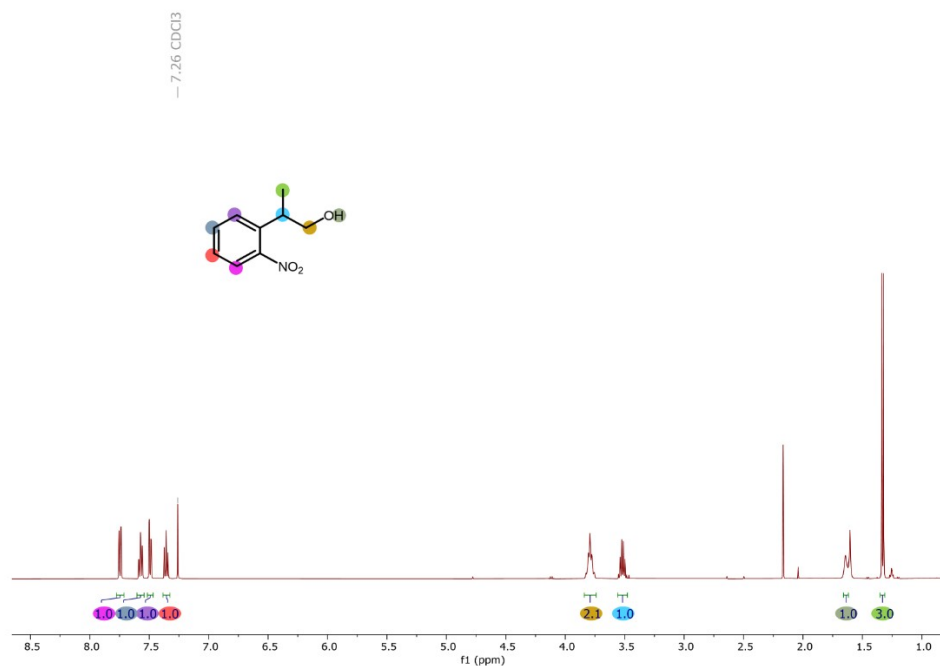


**Figure S4.** <sup>1</sup>H NMR in CDCl<sub>3</sub> of NPPOH.

Triphosgene (1.64 g, 5.52 mmol) in anhydrous THF (30 mL) was cooled to 0 C and a solution of 2-(2-nitrophenyl)propanol (1.0 g, 5.52 mmol) and triethylamine (0.77 mL, 5.52 mmol) was added dropwise. After stirring for 30 minutes at 0C, the reaction was filtered over celite, then THF was removed in vacuo to afford the chloroformate. The chloroformate was then redissolved in dichloromethane (DCM, 20 mL) and slowly added to a solution of 1,1,3,3-tetramethylguanidine (TMG, 0.76 mL, 6.06 mmol) in 30 mL of DCM at 0C. The reaction was stirred at room temperature for 8 hours. The reaction was then neutralized with NaHCO<sub>3</sub> (10% aqueous) and extracted with DCM. The organic phase was dried with MgSO<sub>4</sub>, and solvent removed under vacuum. The product was then purified using silica gel chromatography (DCM/methanol 95:5) to give a yellow oil (Yield: 51%, 910 mg). <sup>1</sup>H NMR (500 MHz, CDCl<sub>3</sub>) δ 7.72 (d, *J* = 7.5 Hz, 1H), 7.57 – 7.49 (m, 2H), 7.31 (ddd, *J* = 8.5, 6.3, 2.5 Hz, 1H), 4.27 (d, *J* = 6.9 Hz, 2H), 3.69 (h, *J* = 6.9 Hz, 1H), 2.81 (s, 12H), 1.36 (d, *J* = 6.9 Hz, 3H). <sup>13</sup>C NMR (125 MHz, CDCl<sub>3</sub>) δ 149.34, 137.27, 131.51, 127.54, 125.97, 123.06, 67.47, 38.77, 32.86, 17.51.

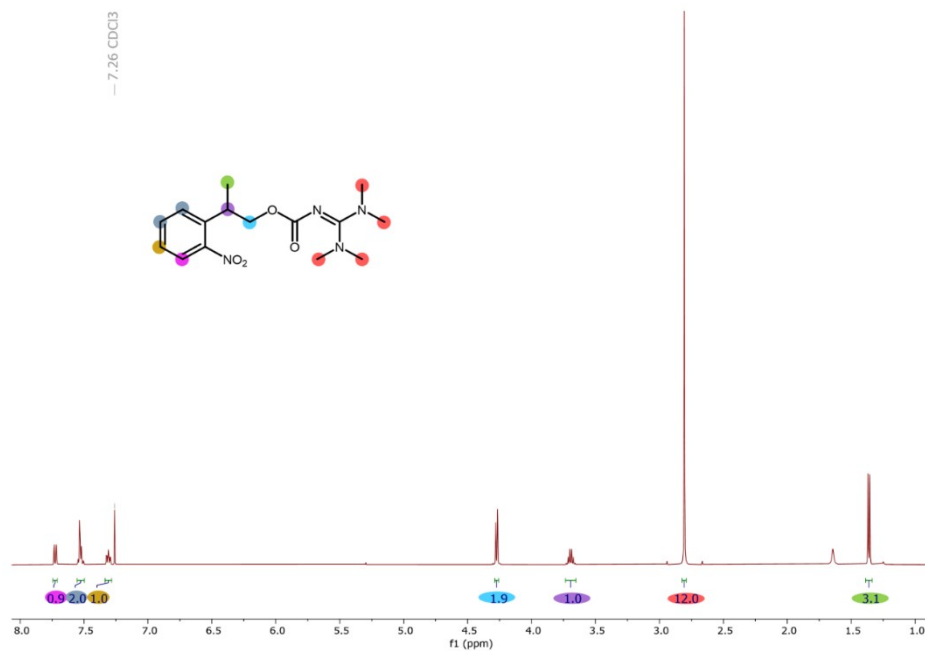


**Figure S5.** <sup>1</sup>H NMR in CDCl<sub>3</sub> of NPPOC-TMG.

## Resin Preparation

Resins were prepared by mixing the PEDGA, PBG, and ionic liquid in the corresponding ratios followed with the addition of the trithiol monomer once the resin was ready to print or test to avoid early polymerization and maintain consistency between experiments. The following is the procedure to prepare the resin used for printing: To make 4 g of resin at 50 wt% ionic liquid 1.3425 g PEDGA, 0.0401 g NPPOC-TMG, and 2.02 g [EBIM] TFSI were mixed until homogenous followed by the addition of 0.6244 g TMPTMP to give 4.029 g resin.

## Rheology

Rheology measurements were conducted on a Discovery HR-2 rheometer from TA instruments. For photorheology experiments, a LED UV-curing accessory centered at 365 nm was used together with an acrylic transparent bottom plate. Photorheology experiments were performed at a frequency of 1 Hz and in the linear viscoelasticity region using 20 mm parallel plates and a gap of 300  $\mu\text{m}$ . In every test, the light was turned on after 30 s equilibration at the targeted shear rate. Stability tests were performed at a constant oscillation strain (5 Pa) over a 3-hour period. Amplitude sweeps were performed at a constant frequency (1.0 Hz) ranging from 0.01% to 100%.

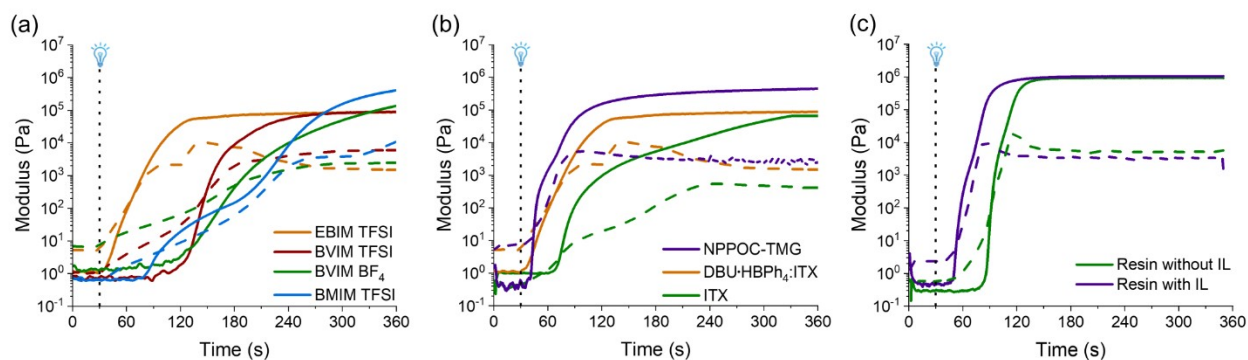


**Figure S6.** Rheology comparing (a) different ionic liquids, (b) different photobase generators, and (c) NPPOC-TMG resin with and without IL.



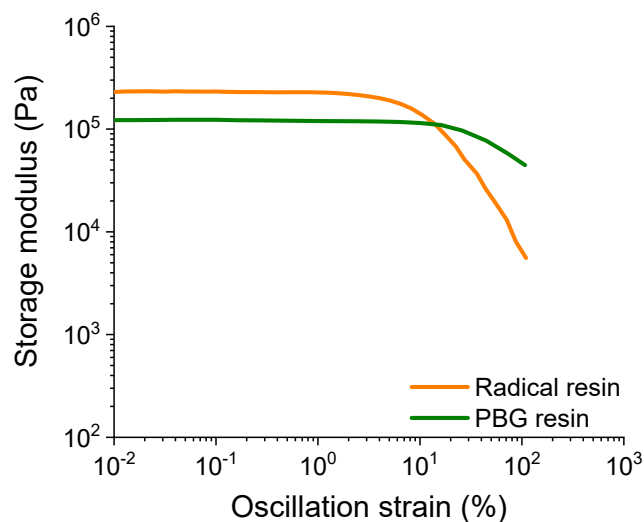


**Figure S7.** Amplitude sweeps of PBG and Radical gels

#### *Photonic Parameters*

Inherent photonic parameters were possible to calculate utilizing the rheometer as well by using the protocol outlined by Rau et al., offering a more analytical determination of the working curve.<sup>7</sup> The Jacob's equations provided the penetration depth ( $D_p$ ) of light in the resin and the critical exposure ( $E_c$ ) derived from the linear regression of the plotted data. The parameters calculated from the rheometer experiment were in high agreement with those obtained from the Asiga printer and digital calipers.

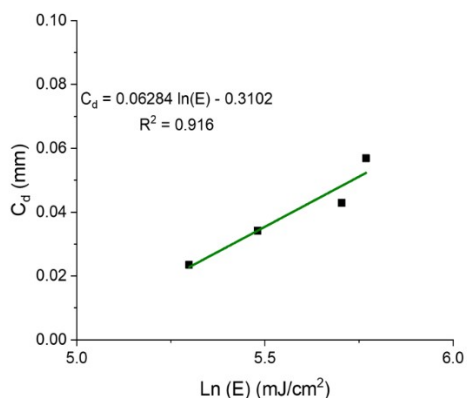


**Figure S8.** Jacob's working curve of the PBG resin obtained from the rheometer at a constant of  $20 \text{ mW cm}^{-1}$ .

#### *UV-Vis Absorption*

UV-Vis spectra were collected on an Agilent Cary 5000 using acetonitrile as the solvent with a spectral range of 200 – 500 nm.

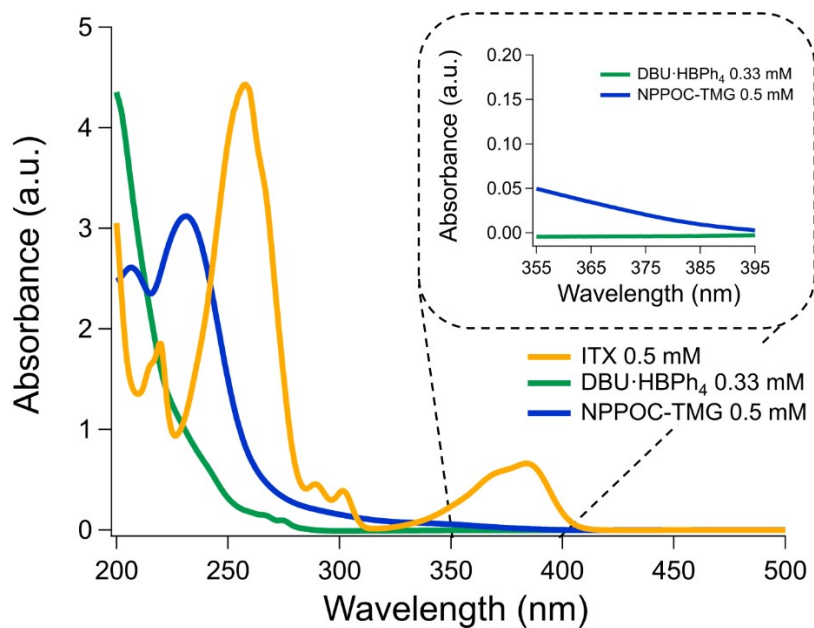


**Figure S9.** UV-vis spectra of photocatalyst with zoom in on 355-395 nm region

*Differential scanning calorimetry*

Differential scanning calorimetry (DSC) measurements were performed using a TA Instruments DSC 250 calorimeter equipped with a TA RCS90 cooling system, using Tzero standard aluminum pans (TA Instruments) and calibrated with an indium standard. The heating and cooling rate for all samples was  $20\text{ }^{\circ}\text{C min}^{-1}$ , except for the final heating cycle, which was run at a rate of  $10\text{ }^{\circ}\text{C min}^{-1}$ .

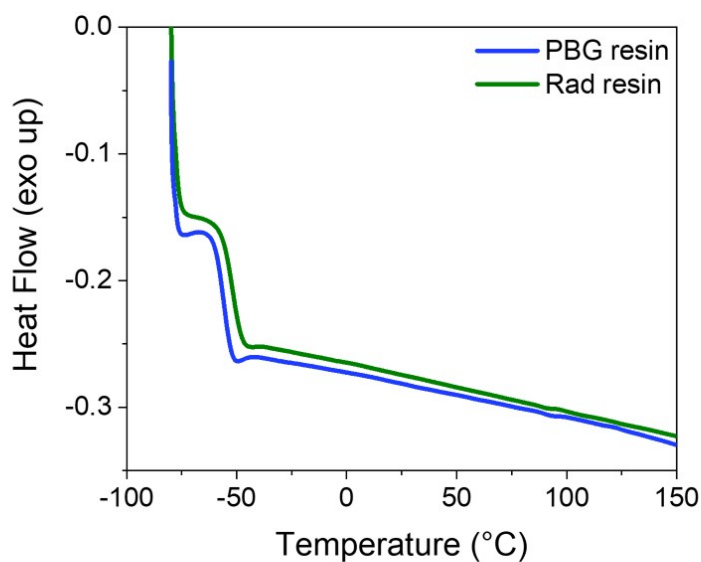


**Figure S10.** DSC curves of radically cured gel vs ionogel cured with a PBG.

*Thermogravimetric analysis*

Thermogravimetric analysis (TGA) was conducted on TA Instruments Q5000. A sample with 25 wt% ionic liquid was used for ease in determining at which temperature the ionic liquid and polymer matrix decomposed. Samples were ramped up at 10 °C min<sup>-1</sup> from 10 to 600 °C under N<sub>2</sub> atmosphere. Decomposition temperature can be determined by the first derivative. At 360 °C about 75 wt% of the mass was lost which is expected to be the polymer matrix and the remaining 25 wt% would be the ionic liquid which decomposed at 450 °C.

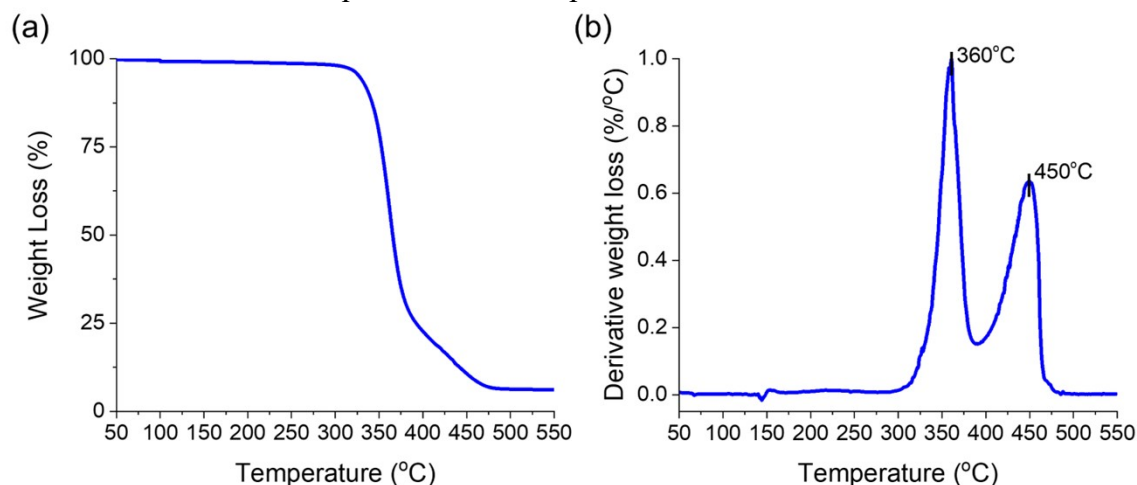


**Figure S11.** TGA of ionogel at 75 wt% polymer, (a) mass lost as sample is heated and (b) the first derivative showing the max temperature during decomposition for each event.

#### Tensile Tests

An Instron 5585H 250 kN electro-mechanical test frame with a 50 N load cell was used to evaluate the tensile properties of the cross-linked ionogel. Printed or cast dogbones specimen followed the specifications of ISO-37 type IV. The printed dogbones were printed using optimized parameters with no post-cure. Casting was done in a Teflon dogbone mold with a glass cover. The cast dogbones were exposed to 385 nm light for 11 min. The chemically cross-linked ionogel was then removed from the mold, flipped, and cured for an additional minute. Each sample was attached to pneumatic self-aligning grips fixed on the load frame, and the sample was subjected to increasing strain at a constant rate of 5 mm/min until mechanical failure of the sample.

**Table S1.** Average results of tensile mechanical data of dogbones from resins

Sample name	Young's Modulus [kPa]	Fracture Strain [mm/mm]	Ultimate Stress [kPa]	Toughness [kJ m <sup>-3</sup> ]
<b>Radical cast 5 min</b>	1394.3 ± 299.1	35.028 ± 7.920	445.39 ± 7.51	81.454 ± 16.399
<b>Radical cast 10 min</b>	1538.8 ± 7.9	24.281 ± 4.506	355.15 ± 60.17	45.741 ± 16.294
<b>Averaged Radical cast</b>	1466.5 ± 191.9	29.655 ± 8.135	400.27 ± 62.77	63.597 ± 24.562
<b>PBG cast 1 min</b>	698.31 ± 34.27	66.001 ± 3.746	365.85 ± 6.28	131.65 ± 7.23
<b>PBG cast 5 min</b>	645.88 ± 1.22	62.161 ± 1.322	334.26 ± 0.20	111.69 ± 3.43
<b>PBG cast 10 min</b>	539.62 ± 57.49	90.836 ± 15.597	373.59 ± 68.45	191.93 ± 70.73

<b>Average PBG cast</b>	616.13 ± 57.49	76.185 ± 17.909	362.27 ± 51.16	154.00 ± 62.21
<b>PBG printed</b>	824.15 ± 73.10	76.88 ± 10.92	496.87 ± 97.46	212.12 ± 70.97

### *Gel Fraction Experiments*

Each sample (~50 mg) was submerged in 10 mL of DCM for 3 d, with the solvent being replaced every 24 h. After the third solvent exchange, the samples were placed in a vacuum oven at 50 °C overnight. The mass of the fully dried sample was subtracted from the original mass of the sample to give the fraction of material that was fully polymerized. The average results are displayed on the table below. The data reveals that the mass loss was due to ionic liquid while the monomers were fully polymerized into the network. FTIR experiments were used to track the conversion of acrylate (810 cm<sup>-1</sup>) and thiol (2570 cm<sup>-1</sup>).

**Table S2.** PBG resin printed dogbones

Sample #	Gel m <sub>i</sub> [g]	Gel m <sub>f</sub> [g]	Gel fraction [%]
1	0.0415	0.0203	49%
2	0.0424	0.0212	50%
3	0.0406	0.0191	47%

**Table S3.** PBG resin cast dogbones

Sample #	Gel m <sub>i</sub> [g]	Gel m <sub>f</sub> [g]	Gel fraction [%]
1	0.0437	0.0217	50%
2	0.0321	0.0154	48%
3	0.0403	0.0200	50%

**Table S4.** Radical resin printed dogbones

Sample #	Gel m <sub>i</sub> [g]	Gel m <sub>f</sub> [g]	Gel fraction [%]
1	0.0581	0.0279	48%
2	0.0647	0.0306	47%
3	0.0355	0.0161	45%

### FTIR experiments

FTIR was collected on a Perkin Elmer Frontier equipped with an ATR crystal. For the liquid resin, a drop was added to the crystal and spectrum was collected. For the cured gels, an 8 mm x 1 mm cylinder was placed on the ATR crystal. The spectrums were all normalized to the same peak at 1730  $\text{cm}^{-1}$  corresponding to the carbonyl peak of the monomers. Thiol consumption was monitored by the S-H resonance at 2560  $\text{cm}^{-1}$  and acrylate consumption was monitored by the CH out-of-plane bending vibration of the vinyl group resonance at 810  $\text{cm}^{-1}$ .

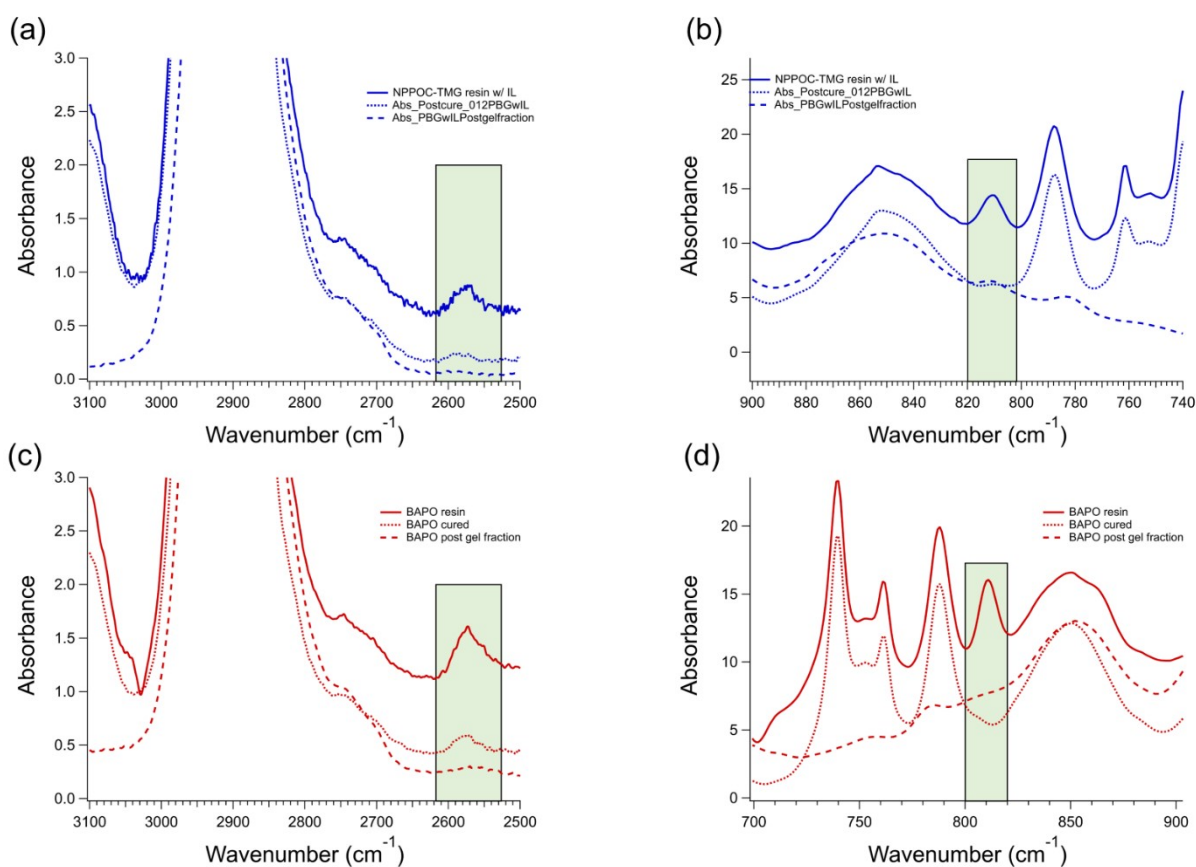


**Figure S12.** FTIR spectra of PBG resin in blue and BAPO resin in red. With zoom-in of the thiol (S-H stretch, 2560  $\text{cm}^{-1}$ ) resonance in graphs (a) and (c) and zoom-in of the acrylate (C-H out-of-plane bending vibration of the vinyl group) resonance in graphs (b) and (d).

### Stress Relaxation Measurements

Relaxation modulus and activation energy was determined by stress relaxation experiments performed in an ARES rheometer (Rheometrics) using a film tension fixture and 5 % of strain at temperatures ranging from 75 °C to 150 °C. The samples used for these measurements had a width between 2.5 to 3 mm and thickness between 0.75 to 1.05 mm. Temperature dependent relaxation times are described by the Arrhenius equation:  $\tau(T) = e^{(E_a/RT)}$ . If stress-relaxation was observed the curves would drop to the line at  $1/e$ .

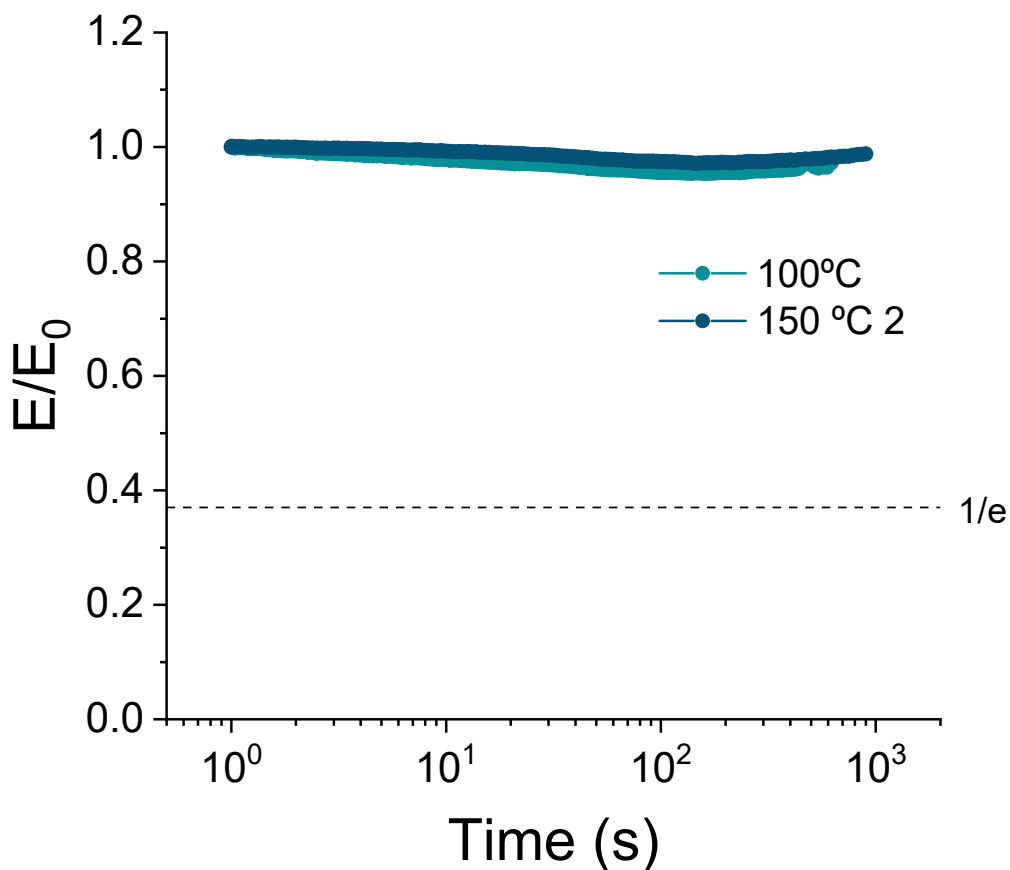


**Figure S13.** Stress-relaxation measurements of photobase generator photopolymerized sample

### Electrical Impedance Spectroscopy

Ionic conductivities were determined by electrochemical impedance spectroscopy (EIS) in an Autolab 302N potentiostat galvanostat at various temperatures (20-100 °C) using a temperature control Microcell HC station. Samples were placed between stainless steel electrodes (surface area = 0.5 cm<sup>2</sup>). The plots were obtained using 10 mV amplitude in the 100 kHz to 1 Hz range.

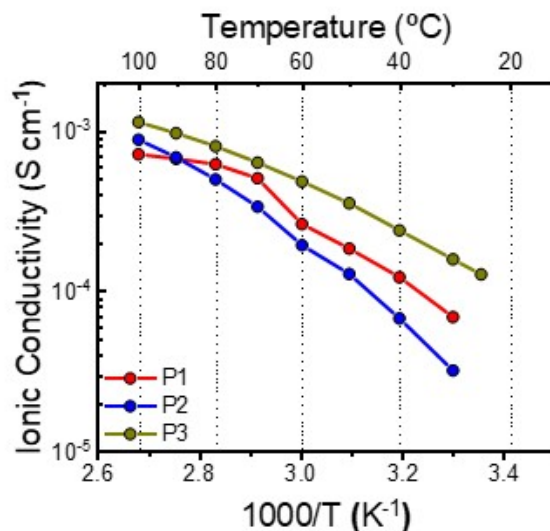


**Figure S14.** EIS of printed ionogel pucks

### Digital Light Processing (DLP) Printing

DLP 3D printing was performed on an Asiga Freefrom Max UV-385 printer equipped with a UV-LED excitation source (385 nm; ~20 mWcm<sup>-1</sup>.) Computer designed 3D objects were prepared for printing in the Asiga Composer software. Designs were printed with one burn-in layer and layer heights of 50 μm. Exposure times for burn-in layers and layers were set to 30 s. The separation velocity was set to 2.500 mm s<sup>-1</sup> and separation distance was set to 2.000 mm.

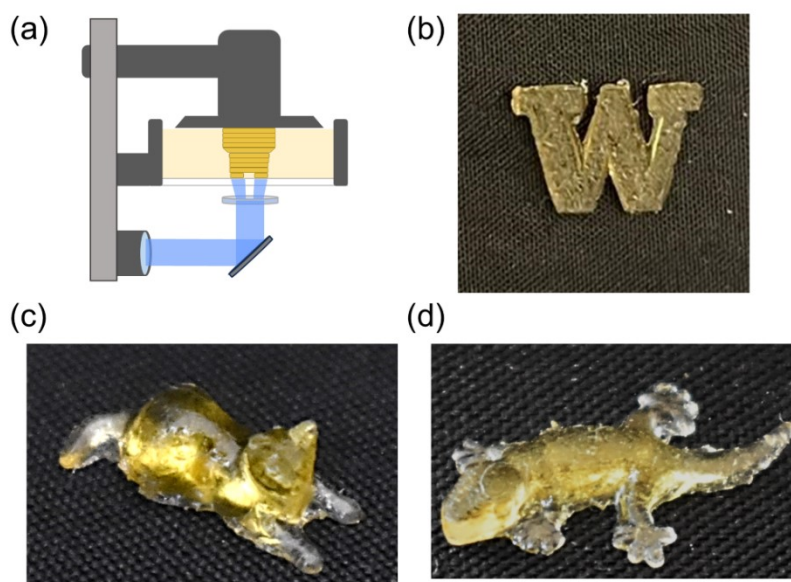


**Figure S15.** Objects were printed on a commercial DLP printer using a resin comprising: 50 wt% [EBIM] TFSI, 2 wt% NPPOC-TMG, 33 wt% PEGDA, and 15 wt% TMPTMP. (a) A diagram of the DLP printer during the printing process. Different shapes were printed, including a (b) “W”, (c) cat, and (d) gecko.



*Keyence microscope images of optimization prints*

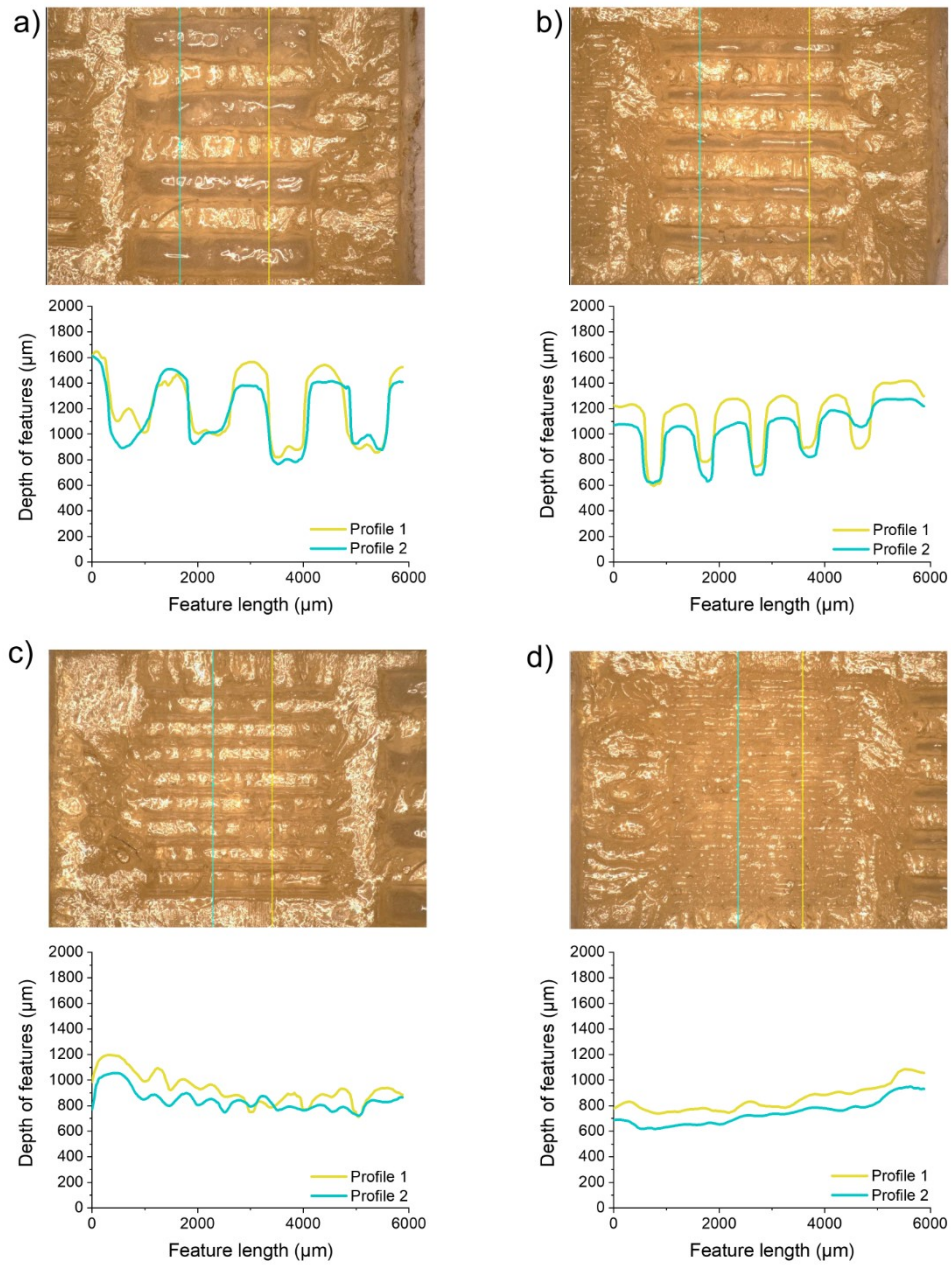


**Figure S16.** Keyence digital microscope images of the printed optimization chip with targeted feature sizes of (a) 1000  $\mu\text{m}$ , (b) 500  $\mu\text{m}$ , (c) 250  $\mu\text{m}$ , and (d) 100  $\mu\text{m}$ .

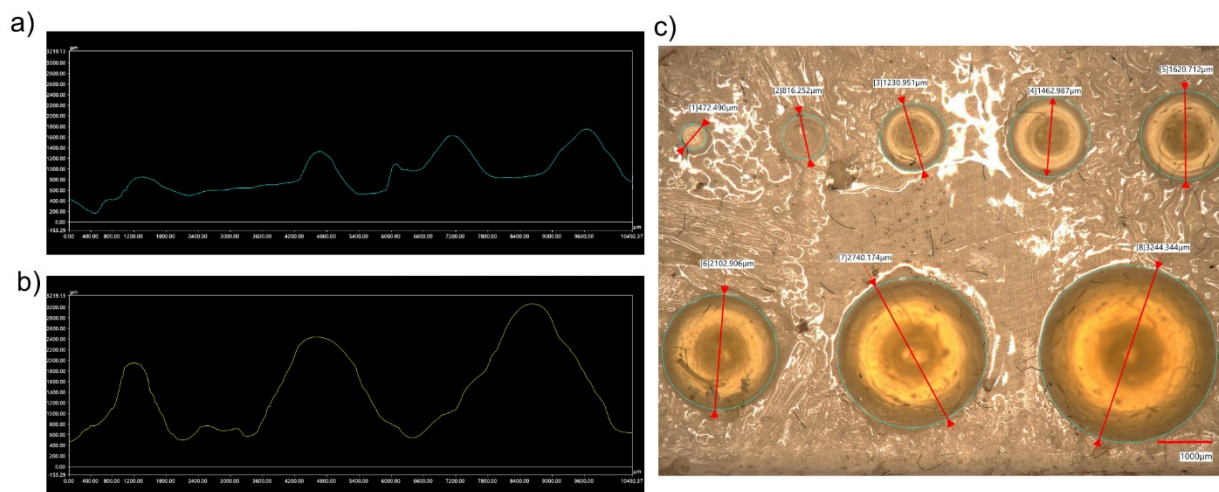


**Figure S17.** Keyence digital microscope images of cones features printed on a flat surface. The cross-sectional profiles are shown with heights of (a) 0.5 – 1.5 mm diameter cones and (b) 2.0 – 3.0 mm diameter cones. (c) The top-down image of the cones.

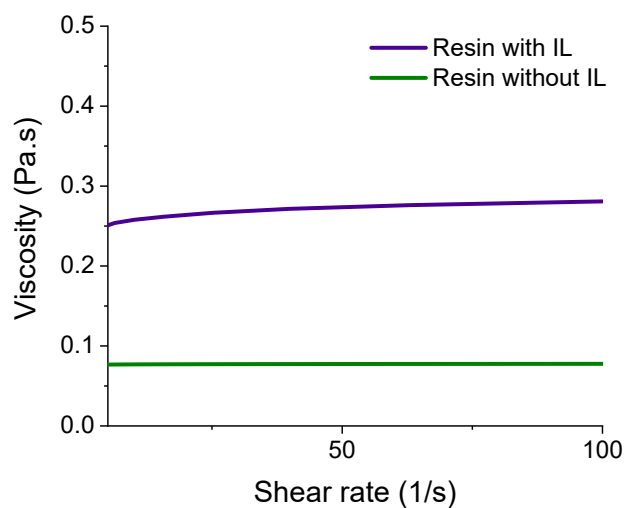


**Figure S18.** Viscosity vs shear rate experiment of NPPOC-TMG resin to determine the effect of ionic liquid (IL).

Works cited:

- (1) Wong, J.; Basu, A.; Wende, M.; Boehler, N.; Nelson, A. Mechano-Activated Objects with Multidirectional Shape Morphing Programmed via 3D Printing. *ACS Appl. Polym. Mater.* **2020**, *2* (7), 2504–2508. <https://doi.org/10.1021/acsapm.0c00588>.

- (2) Wong, J.; Gong, A. T.; Defnet, P. A.; Meabe, L.; Beauchamp, B.; Sweet, R. M.; Sardon, H.; Cobb, C. L.; Nelson, A. 3D Printing Ionogel Auxetic Frameworks for Stretchable Sensors. *Advanced Materials Technologies* **2019**, *4* (9), 1900452. <https://doi.org/10.1002/admt.201900452>.
- (3) Basu, A.; Wong, J.; Cao, B.; Boechler, N.; Boydston, A. J.; Nelson, A. Mechanoactivation of Color and Autonomous Shape Change in 3D-Printed Ionic Polymer Networks. *ACS Appl. Mater. Interfaces* **2021**, *13* (16), 19263–19270. <https://doi.org/10.1021/acsami.1c01166>.
- (4) Sun, X.; Gao, J. P.; Wang, Z. Y. Bicyclic Guanidinium Tetrphenylborate: A Photobase Generator and A Photocatalyst for Living Anionic Ring-Opening Polymerization and Cross-Linking of Polymeric Materials Containing Ester and Hydroxy Groups. *J. Am. Chem. Soc.* **2008**, *130* (26), 8130–8131. <https://doi.org/10.1021/ja802816g>.
- (5) Bhushan, K. R.; DeLisi, C.; Laursen, R. A. Synthesis of Photolabile 2-(2-Nitrophenyl)Propyloxycarbonyl Protected Amino Acids. *Tetrahedron Letters* **2003**, *44* (47), 8585–8588. <https://doi.org/10.1016/j.tetlet.2003.09.155>.
- (6) Zhang, X.; Xi, W.; Huang, S.; Long, K.; Bowman, C. N. Wavelength-Selective Sequential Polymer Network Formation Controlled with a Two-Color Responsive Initiation System. *Macromolecules* **2017**, *50* (15), 5652–5660. <https://doi.org/10.1021/acs.macromol.7b01117>.
- (7) Rau, D. A.; Reynolds, J. P.; Bryant, J. S.; Bortner, M. J.; Williams, C. B. A Rheological Approach for Measuring Cure Depth of Filled and Unfilled Photopolymers at Additive Manufacturing Relevant Length Scales. *Additive Manufacturing* **2022**, *60*, 103207. <https://doi.org/10.1016/j.addma.2022.103207>.